Exploring anti-fibrotic drugs

Luangmonkong, Theerut

Chapter B2

Precision-cut human kidney slices as a model to elucidate the process of renal fibrosis

Elisabeth G.D. Stribos[1,2], Theerut Luangmonkong[2,3], Anna M. Leliveld[4], Igle J. de Jong[4], Willem J. van Son[1], Jan-Luuk Hillebrands[5], Marc A. Seelen[1], Harry van Goor[5], Peter Olinga[2,*,#], Henricus A.M. Mutsaers[2,#]

[1] Department of Internal Medicine, Division of Nephrology, University Medical Center Groningen, the Netherlands

[2] Department of Pharmaceutical Technology and Biopharmacy, University of Groningen, the Netherlands

[3] Department of Pharmacology, Faculty of Pharmacy, Mahidol University, Thailand

[4] Department of Urology, University Medical Center Groningen, the Netherlands

[5] Department of Pathology and Medical Biology, Division of Pathology, University Medical Center Groningen, the Netherlands

* Corresponding author

# Authors contributed equally

Translational Research 2016

Precision-cut human kidney slices as a model to elucidate the process of renal fibrosis

Abstract

Background and purpose

Chronic kidney disease (CKD) is a major health concern and experimental models bridging the gap between animal studies and clinical research are currently lacking. Here, we evaluated precision-cut human kidney slices (PCKS) as a potential model for renal disease.

Experimental approach

PCKS were prepared from human cortical tissue obtained from tumor-nephrectomies and cultured up to 96h. Morphology, cell viability and metabolic functionality (*i.e.* UDP-glucuronosyltransferase and transporter activity) were determined to assess PCKS integrity. Furthermore, inflammatory- and fibrosis-related gene expression was characterized. Finally, to validate the model, renal fibrogenesis was induced using transforming growth factor beta 1 (TGF-β1).

Key results

Preparation of PCKS induced an inflammatory tissue response, while long-term incubation (96h) induced fibrogenesis as seen by an increased expression of collagen type 1A1 (COL1A1) and fibronectin (FN1). Importantly, PCKS remained functional for more than 48h as evidenced by active glucuronidation and phenolsulfonphthalein uptake. In addition, cellular diversity appeared to be maintained, yet we observed a clear loss of nephrin mRNA levels suggesting that our model might not be suitable to study the role of podocytes in renal pathology. Moreover, TGF-β1 exposure augmented fibrosis, as illustrated by an increased expression of multiple fibrosis markers including COL1A1, FN1 and alpha smooth muscle actin.

Conclusion and implications

PCKS maintain their renal phenotype during culture and appear to be a promising model to investigate renal diseases *e.g.* renal fibrosis. Moreover, the human origin of PCKS makes this model very suitable for translational research.

Key words: *ex vivo*; *in vitro*; human; renal fibrosis.

Abbreviations: 7-HCG, 7-hydroxycoumarin glucuronide; BCRP, breast cancer resistance protein; CKD, chronic kidney disease; COL1A1, collagen 1A1; ECM, extracellular matrix; ESRD, end-stage renal disease; FN1, fibronectin 1; HSP47, heat shock protein 47; OAT, organic anion transporter; OATP4C1, organic anion transporting polypeptide 4C1; PAI, plasminogen activator inhibitor; PCKS, precision-cut kidney slices; PDGFB, platelet-derived growth factor subunit B; TGF-β1, transforming growth factor beta 1; UGT, UDP-glucuronosyltransferase; αSMA, alpha smooth muscle actin.

Introduction

Chronic kidney disease (CKD) affects approximately 10% of the adult population in developed countries [1]. CKD is irreversible and can progress to end-stage renal disease (ESRD), demanding renal replacement therapy. Yet, at this time, no effective therapy exists to halt CKD progression. Loss of functional tissue due to glomerular and tubulointerstitial accumulation of extracellular matrix (ECM) proteins, *i.e.* fibrosis, is a key event in the development and perpetuation of CKD [2]. Currently, therapies for organ fibrosis in CKD patients solely focus on the origin of renal failure, *e.g.* diabetes or hypertension, and consequently have limited potential in halting fibrosis [3, 4]. Therefore, insight into renal fibrogenesis might aid in the development of therapeutic approaches to prevent loss of kidney function [5], or even reverse fibrosis.

Fibrosis is a complex pathophysiological process encompassing a myriad of cells and signaling pathways. A multitude of triggers can initiate the fibrotic response, including proteinuria and glomerular IgA deposition, yet irrespective of the initial insult, it will ultimately result in loss of organ architecture and function [4, 6]. Transforming growth factor beta 1 (TGF-β1) is one of the key factors involved in fibrogenesis, and activation of the TGF-β1 signaling pathway will increase the expression of, among others, plasminogen activator inhibitor (PAI)-1. This glycoprotein is a powerful promoter of renal fibrosis and is associated with many aggressive kidney diseases [7]. Even though there is great body of literature regarding fibrosis, the fibrotic process is still not understood completely. To elucidate the mechanisms of renal fibrosis, there is an urgent need for reliable models mimicking the human *in vivo* situation. Results obtained with existing animal models differ per strain [8], and *in vitro* models fail to replicate the multicellular nature of the fibrotic process. Recently, Poosti *et al.*, reported the use of murine precision-cut kidney slices (PCKS) as a suitable model to investigate renal fibrosis [9]. PCKS are ideal to study multicellular (pathological) processes, *e.g.* fibrosis, since cellular diversity as well as organ architecture is maintained in the slices. In the current study, we aimed to improve the PCKS model by preparing slices from human tissue, and we established and characterized human PCKS as a unique *ex vivo/in vitro* model for renal disease.

Methods

Ethics statement

This study was approved by the Medical Ethical Committee of the University Medical Centre Groningen (UMCG), according to Dutch legislation and the Code of Conduct for dealing responsibly with human tissue in the context of health research (www.federa.org), refraining the need of written consent for 'further use' of coded-anonymous human tissue. The procedures were carried out in accordance with the experimental protocols approved by the Medical Ethical Committee of the UMCG.

Renal tissue

Macroscopically healthy renal cortical tissue from tumor-nephrectomies was obtained and kept in ice-cold University of Wisconsin solution. Cold ischemia time between nephrectomy and culturing was limited to 2h. Patient demographics are presented in Table 1.

Table 1: Patient demographics.

Characteristic	Value
Gender (%, female)	50.0
Age (mean, years)	55.1 ± 21.3
Nephrectomy side (%, right)	100.0
Serum creatinine before nephrectomy (mean, µmol/L)	80.2 ± 11.3
eGFR before nephrectomy (mean, mL/min/1.73 m²)*	77.8 ± 9.4

*Calculated using the Modification of Diet in Renal Disease (MDRD) formula. Values are presented as means ± standard deviation or otherwise if indicated (n=6).

Preparation/characterization of PCKS

Workflow of PCKS preparation is shown in Figure 1. In short, cylindrical cores, 6 mm in diameter, were obtained from human renal tissue using a biopsy punch. Kidney slices were subsequently prepared in ice-cold Krebs-Henseleit buffer, supplemented with 25 mM D-glucose (Merck, Darmstadt, Germany), 25 mM $NaHCO_3$ (Merck), 10 mM HEPES (MP Biomedicals, Aurora, US) and saturated with carbogen (95% O_2/5% CO_2), using a Krumdieck tissue slicer as previously described [10]. PCKS, with a wet weight of 4-6 mg and an estimated thickness of 250-300 µm, were incubated individually in 1.3 mL of Williams medium E with Glutamax (Life Technologies, Carlsbad, US) containing 10 µg/mL ciprofloxacin and 2.7 g/L D-(+)-Glucose solution (Sigma, Saint Louis, US) at 37 °C in a 80% O_2/5% CO_2 atmosphere, while gently shaken [10]. Medium was refreshed every 24h.

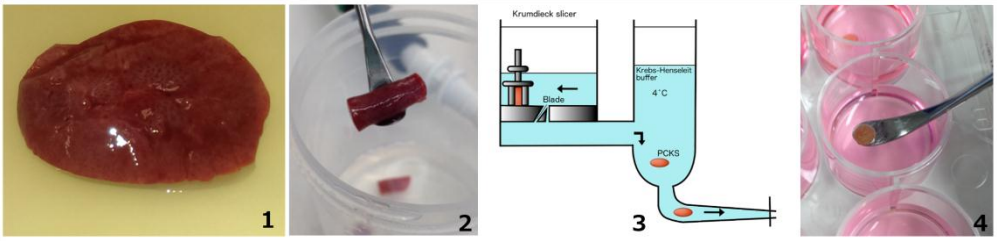

Figure 1: Workflow preparation of precision-cut kidney slices. Cylindrical cores, 6 mm in diameter, were obtained from human renal cortical tissue using a biopsy punch (Step 1, 2). PCKS were prepared using the Krumdieck tissue slicer, slices with a wet weight of 4-6 mg had an estimated thickness of 250-300 µm (Step 3, 4). Slices were subsequently incubated in optimized medium at 37 °C and 80% O_2/5% CO_2 in an incubator shaking at 90 rpm (amplitude 2 cm).

For immunohistochemistry, PCKS were fixed in 10% formalin, embedded in paraffin and sectioned (2 µm) followed by PAS staining to assess morphology or Sirius red staining to visualize collagen protein expression. PCKS diameter was measured using ImageJ (US National Institutes of Health).

Viability was determined by both ATP content as previously described [11] and LDH release using the CytoTox-ONE Homogenous Membrane Integrity assay (Promega, Madison, US).

PCKS functionality

UGT activity was measured by HPLC. Following incubation, PCKS were incubated with 0.5 mM 7-hydroxycoumarin (7-HC) for 3h at 37°C. Afterwards, aliquots of culture medium were centrifuged (12,470 g, 5 minutes) and injected into the HPLC system (PE-Sciex API 3000, Concord, Canada) equipped with a C18 column (150 x 2.1 mm, 5 µm, Alltech Associates, Deerfield, US). 7-HC metabolites were measured as previously described [12].

To determine phenolsulfonphthalein uptake, slices were cultured as described above and subsequently homogenized in sonication solution, containing 70% ethanol and 2 mM EDTA, using a Mini-Beadbeater, and extinction of the solution was measured at 558 nm using a spectrophotometer (Synergy HT BioTek, Winooski, US).

Quantitative PCR

Total RNA from untreated or exposed (5 ng/mL human TGF-β1; Roche, Basel, Switzerland) PCKS was isolated with the RNeasy mini kit (Qiagen, Venlo, the Netherlands), using a Mini-Beadbeater for homogenization. RNA (1 µg) was reverse transcribed using the Reverse Transcription System (Promega). Subsequently, cDNA was used for RT-qPCR performed with a 7900HT RT-qPCR system (Applied Biosystems). Relative expression values were expressed as percentage compared to GAPDH (100%) or as fold induction using the $2^{-\Delta\Delta Ct}$ method. Used primers are listed in Table 2.

Table 2: Primers used in quantitative real-time PCR.

Sequence of primers and probes (Sigma)			
Gene	**Forward**	**Reverse**	**Probe**
αSMA	AGGGGGTGATGGTGGGAA	ATGATGCCATGTTCTATCGG	GGGTGACGAAGCACAGAGCA
FN1	AGGCTTGAACCAACCTACGGATGA	GCCTAAGCACTGGCACAACAGTTT	ATGCCGTTGGAGATGAGTGGGAA
GAPDH	ACCAGGGCTGCTTTTAACTCT	GGTGCCATGGAATTTGCC	TGCCATCAATGACCCCTTCA
HSP47	GCCCACCGTGGTGCCGCA	GCCAGGGCCGCCTCCAGGAG	CTCCCTCCTGCTTCTCAGCG
COL1A1	CAATCACCTGCGTACAGAACGCC	CGGCAGGGCTCGGGTTTC	CAGGTACCATGACCGAGACGTG
PAI-1	CACGAGTCTTTCAGACCAAG	AGGCAAATGTCTTCTCTTCC	_

Custom primers & TaqMan probes (Applied Biosystems)			
Gene	**Assay ID**	**Gene**	**Assay ID**
BCRP	Hs01053790_m1	***OAT1***	Hs00537914_m1
CD31	Hs00169777_m1	***OATP4C1***	Hs00698884_m1
E-cadherin	Hs01023894_m1	***PDGFB***	Hs00966522_m1
IL-1β	Hs01555410_m1	***TGF-β1***	Hs00998133_m1
IL-6	Hs00985639_m1	***UGT1A1***	Hs02511055_s1
IL-8	Hs00174103_m1	***UGT1A9***	Hs02516855_sH
Nephrin	Hs00190446_m1	***Vimentin***	Hs00185584_m1

Western blot

Total protein (100 µg) was separated via SDS/PAGE using 10% gels and blotted onto PVDF membranes. Antibodies used are listed in Table 3. Proteins bands were visualized using the VisiGlo Prime HRP Chemiluminescent Substrate Kit (Amresco, Solon, US).

Table 3: Antibodies used in Western blotting.

Antibody and dilution	Manufacturer
Anti-collagen type I (COL1), 1:1000	Rockland, Pennsylvania, US
Anti-glyceraldehyde-3-phosphate dehydrogenase (GAPDH), 1:5000	Sigma, Saint Louis, US
Polyclonal goat anti-rabbit immunoglobulins/HRP, 1:2000	Dako, Glostrup, Denmark
Polyclonal rabbit anti-mouse immunoglobulins/HRP, 1:5000	Dako, Glostrup, Denmark

Statistics

Statistics were performed using Graphpad Prism 6.0 by either a Kruskal-Wallis test followed by Dunn's multiple comparisons test or the Mann-Whitney test as appropriate. Differences between groups were considered to be statistically significant when $p<0.05$.

Results and discussion

Characterization of PCKS

Figure 2A shows the morphology of PCKS during incubation. As demonstrated, general morphology remains good between 3-72h with only minor signs of cellular damage (*e.g.* pyknosis and anucleosis). Closing of tubuli was also observed probably due to a lack of pre-urine flow. Furthermore, PCKS became smaller during culture (Figure 2B and 2C).

Next, viability of PCKS was assessed by ATP content and LDH leakage. ATP levels greatly increased at the start of incubation, from 4.1 (0h) to 16.6 pmol/µg (3h; Figure 2D), in line with previous observations in liver slices [13]. Furthermore, ATP levels remained fairly stable during culture with a content of 11.2 pmol/µg at 96h. LDH levels in the culture medium were also constant (Figure 2E) indicating that PCKS remained viable. These finding are in agreement with the study from Poosti *et al*. showing that murine PCKS are viable up to 72h [9].

Metabolic activity and cell marker expression during incubation

The kidney contributes greatly to metabolism and (transporter-mediated) solute clearance [14]. Therefore, we studied transporter activity and UDP-glucuronosyltransferase (UGT) functionality. Uptake of phenolsulfonphthalein, an organic anion transporter (OAT) substrate [15], was observed at 3-48h and OAT activity time-dependently decreased with 94% between 3-96h (Figure 3A), in line with the observed OAT1 gene expression ($r=0.68$, $p<0.001$). Furthermore, we observed mitigated expression of organic anion transporting polypeptide 4C1 (OATP4C1) and breast cancer resistance protein (BCRP) at the start of culture (0-24h), after which levels remained stable. These findings are in agreement with *in vitro* studies performed with primary human proximal tubular epithelial cells (PTECs), in which functional expression of OATs can be sustained for a limited time [16].

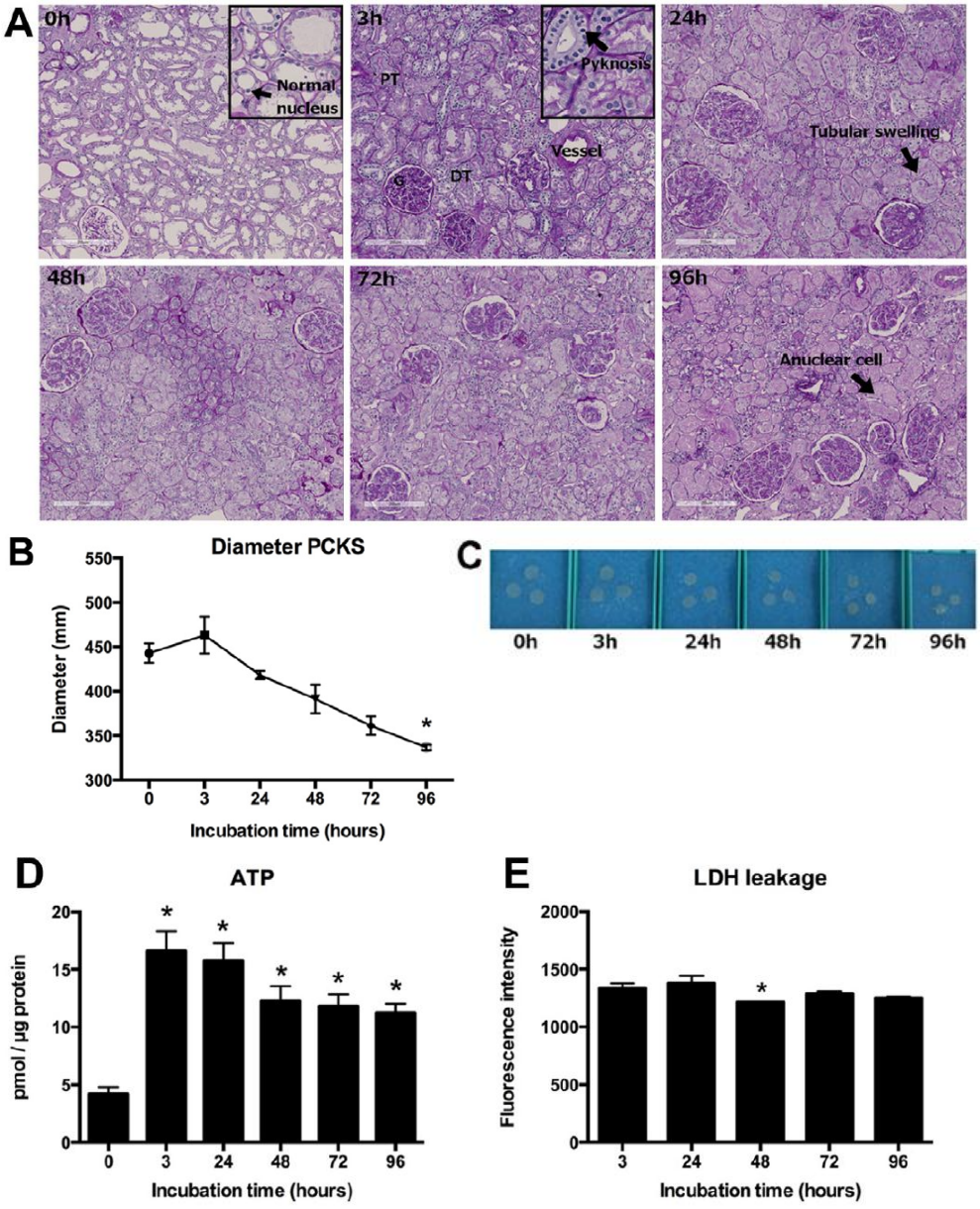

Figure 2: General morphology and viability of PCKS. (A) PAS staining of PCKS during culture, magnification 10X; Insets, magnification 20X (B, C) Representative figures and quantification of PCKS size during incubation, quantified using ImageJ (n=3). (D, E) Viability of PCKS was assessed by ATP content and LDH leakage. Data are presented as means ± SEM of minimally five independent experiments performed in triplicate. Statistical analysis was performed via a Kruskal-Wallis test followed by Dunn's multiple comparisons, compared to first column. *p<0.05.

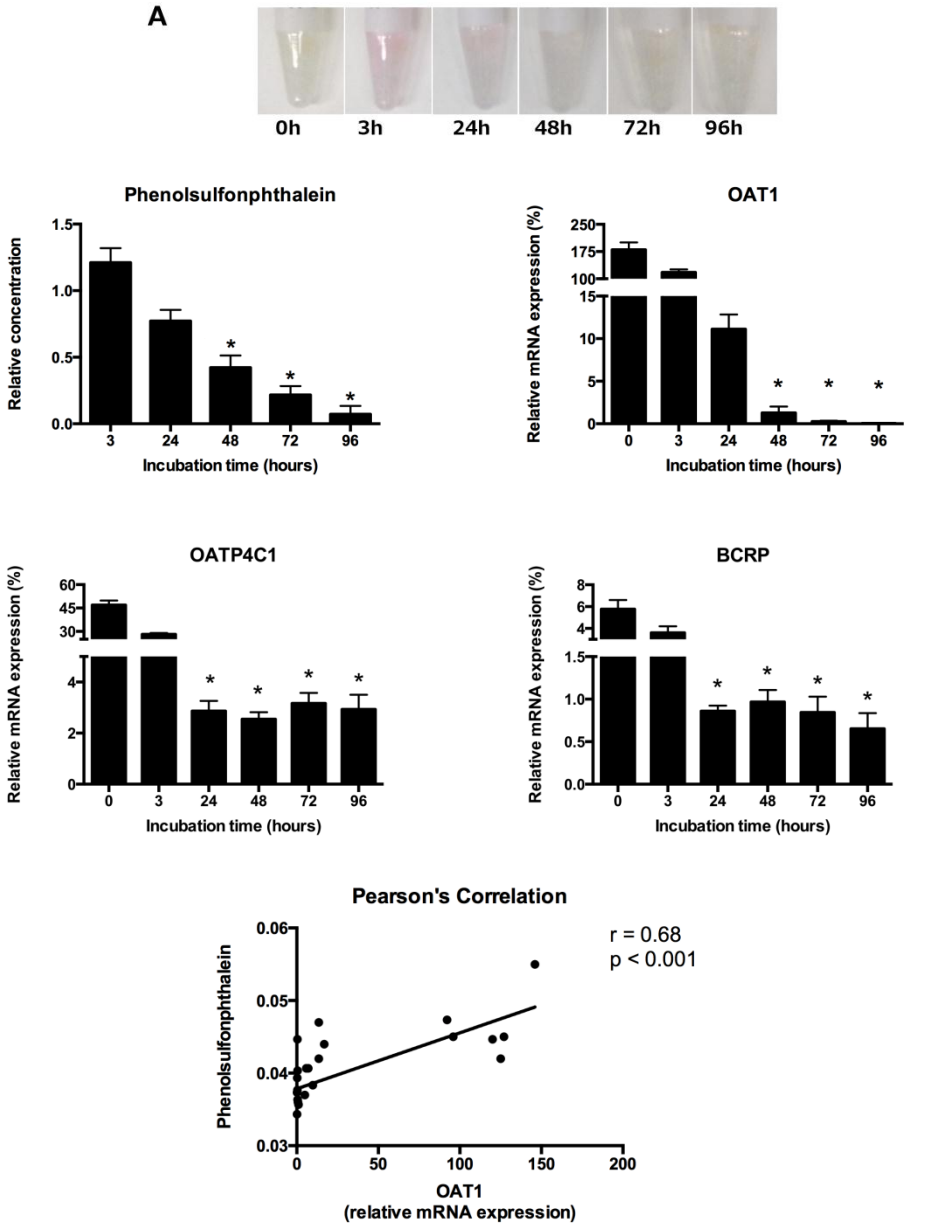

Figure 3: Functionality and cellular changes during culture of PCKS. (A) Representative figures and quantification of phenolsulfonphthalein uptake in PCKS determined by a spectrophotometer at 558 nm. (B) Enzyme activity was determined by HPLC. Slices were incubated with 7-HC (0.5 mM) for 3h at 37 °C. (A, B, C) Gene expression was studied by RT-qPCR. Relative expression was calculated using the housekeeping gene GAPDH (100%). Data are presented as means ± SEM of six independent experiments performed in triplicate. Statistical analysis was performed via a Kruskal-Wallis test followed by Dunn's multiple comparisons test, compared to first column. *p<0.05.

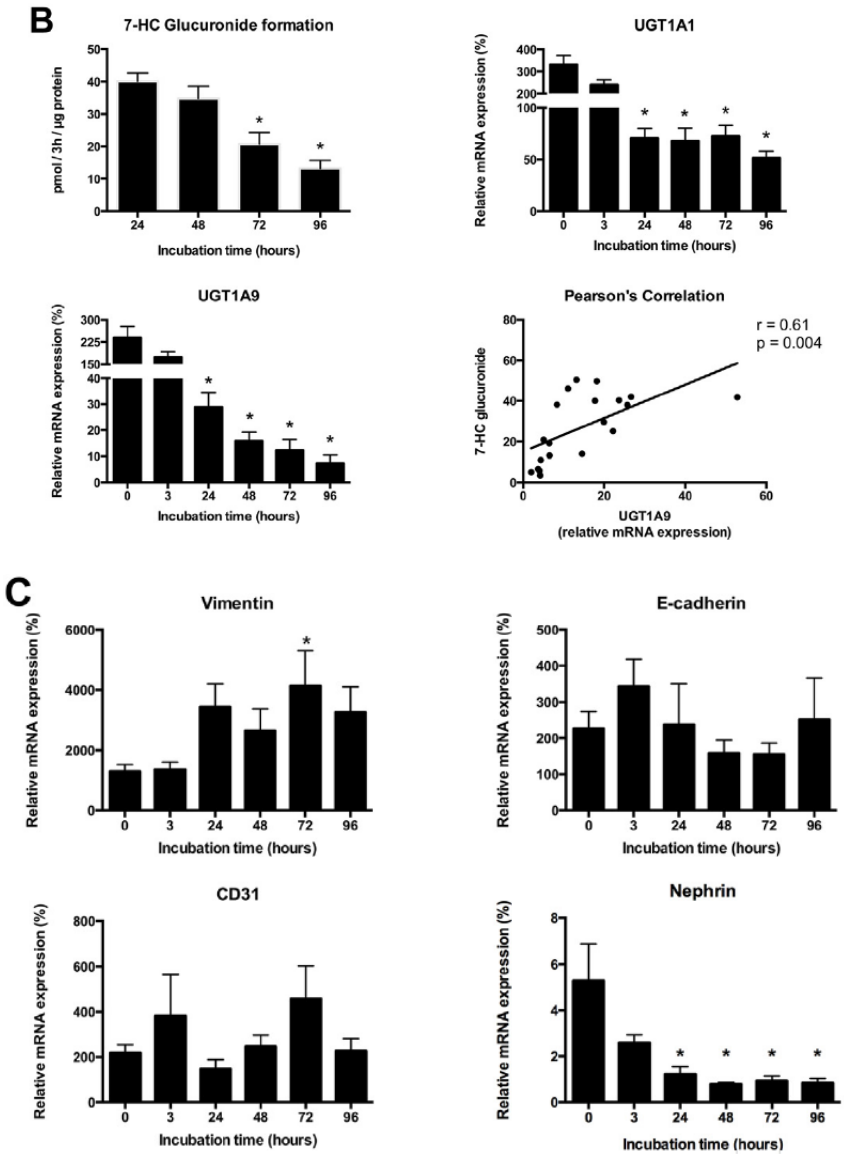

Figure 3: Continued from previous page.

Furthermore, 7-hydroxycoumarin glucuronide (7-HCG) formation was observed in PCKS for more than 48h. Glucuronidation time-dependently decreased from 40.1 (24h) to 13.2 pmol/3h/µg at 96h (Figure 3B). Moreover, UGT activity clearly correlated with UGT1A9 gene expression (r=0.61, p=0.004), a main contributor to renal glucuronidation [17]. In addition, similar to OATP4C1 and BCRP, UGT1A1 expression diminished from 0-24h, after which it stayed constant. Previously, de Kanter *et al*. demonstrated UGT activity in human PCKS during short-term (3h) incubation [12]. Here, we show long-term functionality of UGTs in PCKS, suggesting that the model is suitable for metabolism studies.

Moreover, no clear differences were observed in gene expression of vimentin, e-cadherin and CD31 during culturing (Figure 3C), suggesting that (myo)fibroblasts, epithelial cells and endothelial cells, respectively, were not lost during incubation. Of note, even though CD31 is a well-established marker for endothelial cells [18], under pathological conditions pro-fibrotic renal fibroblasts can also express CD31 [19]. Furthermore, we observed a marked decrease in the expression of nephrin, a podocyte marker and key component of the slit diaphragm (Figure 3C) [20]. Lower nephrin levels indicate dedifferentiation or damage of podocytes, possibly induced by platelet-derived growth factor [21], yet it does not necessarily correlate with podocyte apoptosis [22]. Thus, the fate of podocytes in our model remains to be fully characterized.

Taken together, PCKS behave similar to PTECs during culture, yet the major advantage of our model is that it appears to mimic and retain the cellular and architectural complexity of the kidney.

Expression of inflammatory and fibrosis markers during incubation

To assess the effect of slicing on cell stress, IL-6, IL-8 and IL-1β gene expression was determined. Expression of all three interleukins markedly increased from 4.5% to more than 130% in the beginning of culturing (3-24h), whereafter gene expression decreased (Figure 4A). These findings suggest that an early inflammatory response is evoked in PCKS, still the trigger for the observed increase remains unclear.

With regards to fibrogenesis, we observed a marked increase in the gene expression of collagen 1A1 (COL1A1) and fibronectin 1 (FN1) as well as elevated type I collagen protein levels during culture (Figure 4B and 4C). The observed effect was concurrent with an increased gene expression of TGF-β1. Furthermore, we detected elevated gene levels of platelet-derived growth factor subunit B (PDGFB) at 3h. Thus, the observed fibrotic response in PCKS is likely caused by a concerted action of the TGF-β1 and PDGF pathways possibly activated by interleukins. This notion is in line with previous studies showing that mechanical stress and cytokines, among other factors, drive a fibrogenic response [23]. In contrast, gene expression of alpha smooth muscle actin (αSMA), a marker for matrix producing myofibroblasts [24], first diminished from 38.4% (0h) to 5.0% (24h) and subsequently increased (12.4%; 96h), while no changes were observed in the expression of heat shock protein 47 (HSP47). A similar expression profile is shown in human liver slices [13]. Thus, the collagen-producing cells in PCKS remain to be identified.

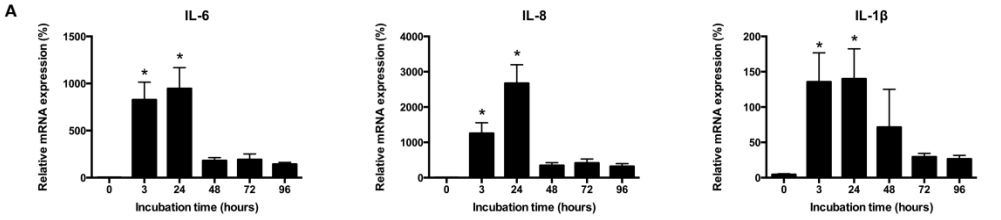

Figure 4: Continued on next page.

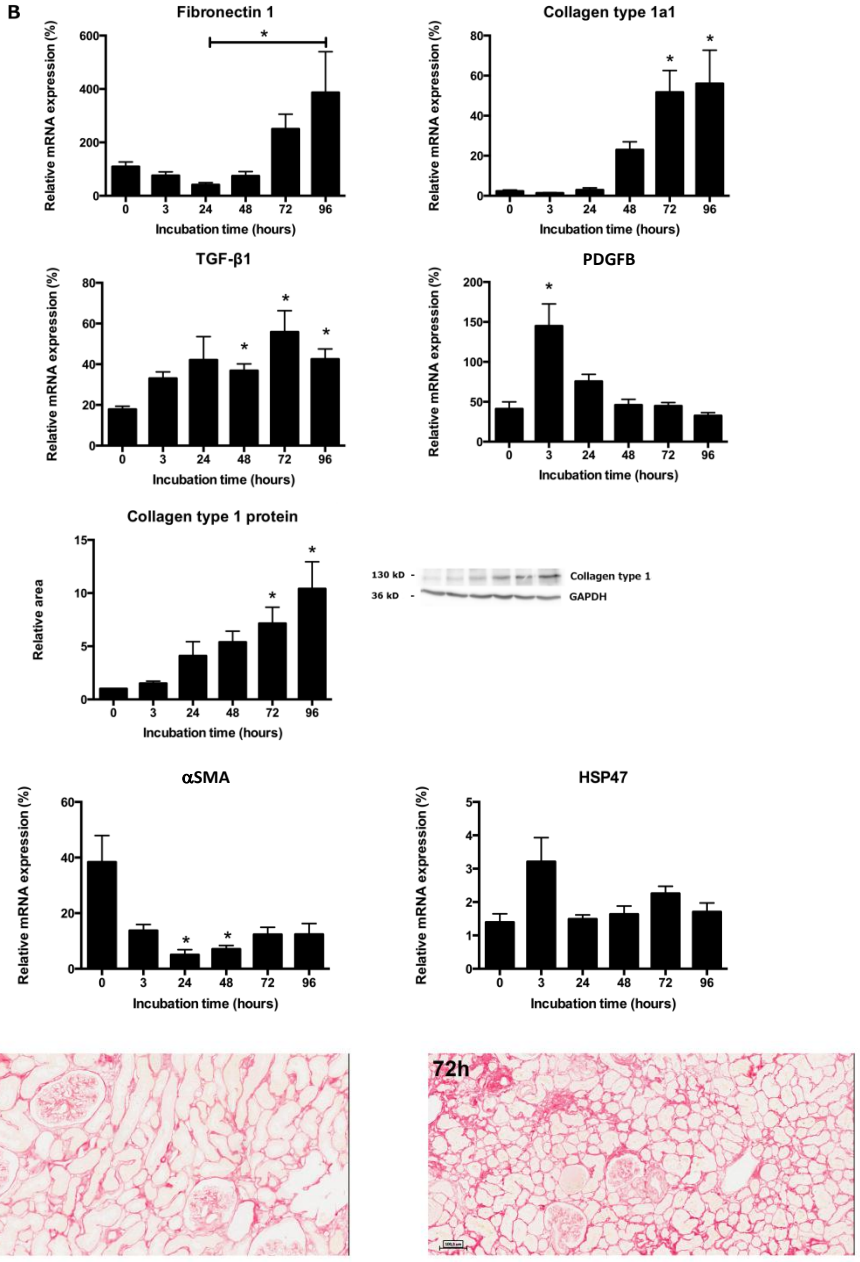

Figure 4: Expression of inflammatory and fibrosis markers during incubation of PCKS. (A, B) Gene expression was studied by RT-qPCR. Relative expression was calculated using the household gene GAPDH (100%). Data are presented as means ± SEM of six independent experiments performed in triplicate. Collagen type 1 protein expression was studied using Western blot (n=3). Statistical analysis was performed via a Kruskal-Wallis test followed by Dunn's multiple comparisons test, compared to 0h. *p<0.05. (C) Sirius red staining of PCKS during culture, magnification 20X.

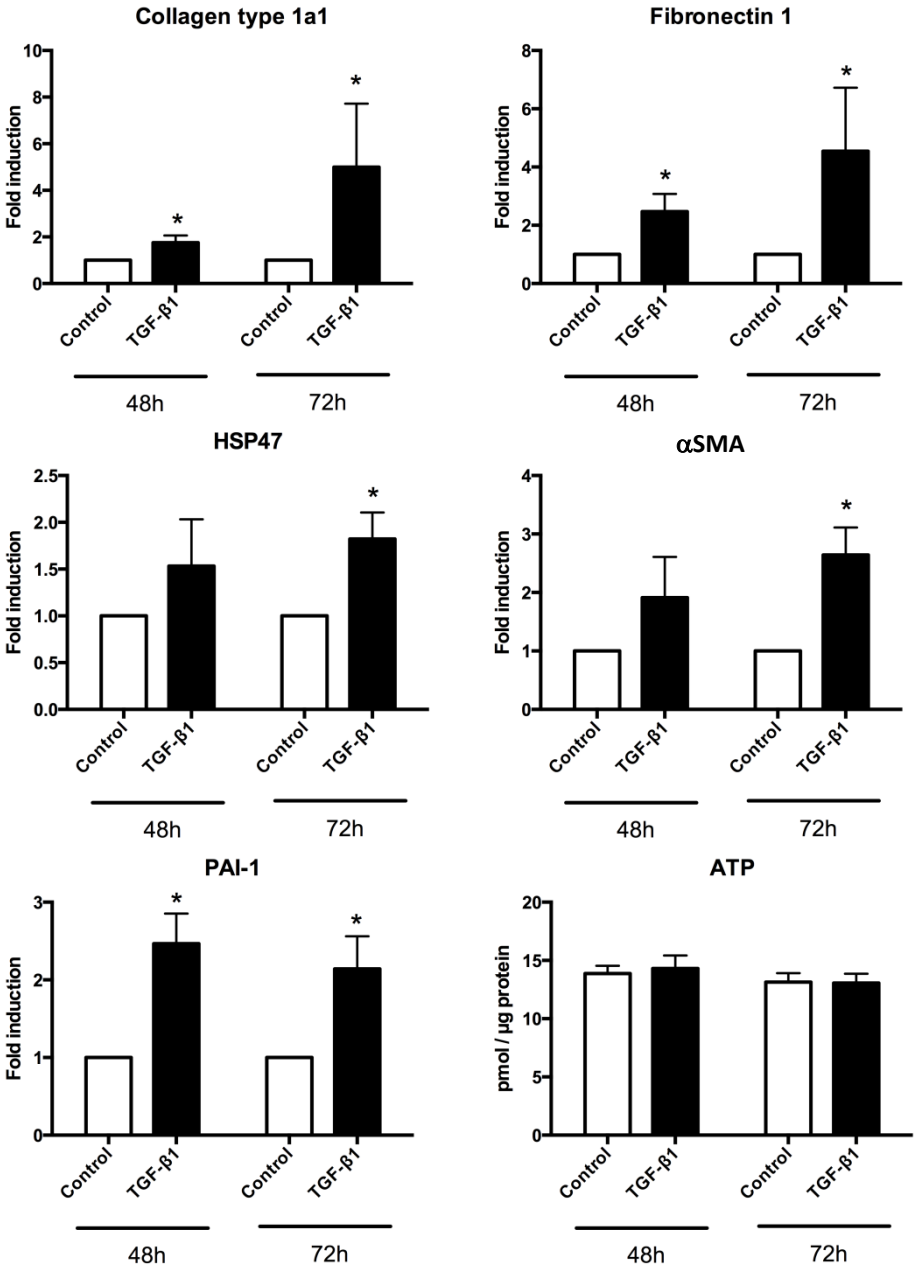

Figure 5: Induction of renal fibrosis with TGF-β1. PCKS were treated with 5 ng/mL human TGF-β1 for either 48 or 72h. Subsequently, gene expression was studied by RT-qPCR, expressed as fold induction using the $2^{-\Delta\Delta Ct}$ method, and viability was assessed by ATP content of the slices. Data are presented as means ± SEM of four independent experiments performed in triplicate. Groups were compared to control using the Mann-Whitney test. *p<0.05.

PCKS as a model for renal fibrosis

Lastly, we investigated whether the fibrotic response could be augmented in PCKS. Therefore, we exposed PCKS to TGF-β1, a key mediator of fibrosis [25, 26]. As shown in Figure 5, treatment with TGF-β1 for 48h significantly increased the fibrogenic response, resulting in a more than 1.8-fold increase in gene expression of COL1A1 and FN1, similar to the observations in murine PCKS [9]. Moreover, exposure to TGF-β1 for 72h significantly augmented the gene levels of all the tested fibrosis markers namely COL1A1, FN1, HSP47 and αSMA, without affecting PCKS viability (Figure 5). Moreover, we observed an increased expression of PAI-1, a downstream signaling molecule of the TGF-β1 pathway, indicating successful activation of the TGF-β1 signaling cascade in human PCKS. Therefore, our model can be used to investigate renal fibrogenesis and the underlying molecular pathways.

Conclusion

In conclusion, we have characterized a unique *ex vivo/in vitro* model to investigate human renal disease, *viz*. precision-cut kidney slices. Merits of this model are the human origin of the tissue and the fact that original organ architecture is maintained. A limitation of the model is that circulating bone marrow-derived cells that contribute to the pathogenesis of fibrosis, *e.g.* macrophages [27], are absent. In addition, the observed loss of differentiated podocytes indicates that our model is not suitable to study podocyte injury and loss as factors in renal pathology. Still, the current study with human PCKS paves the way for a myriad of novel avenues of research including unraveling the molecular mechanism of human renal fibrosis and CKD progression as well as identifying potential anti-fibrotics. The latter might even be tested in PCKS prepared from diseased (*i.e.* fibrotic) instead of healthy renal tissue.

Acknowledgements

This work was supported by ZonMw (the Netherlands Organization for Health Research and Development), grant number 114021010. The authors thank M.M. Dekker and S. Suriguga for technical assistance with the morphology experiments, M.H. de Jager for performing the HPLC measurements and J.P. Arends, MD, for his expertise in microbiology.

References

1. James, M.T., B.R. Hemmelgarn, and M. Tonelli, Early recognition and prevention of chronic kidney disease. Lancet, 2010. 375(9722): p. 1296-309.
2. Decleves, A.E. and K. Sharma, Novel targets of antifibrotic and anti-inflammatory treatment in CKD. Nat Rev Nephrol, 2014. 10(5): p. 257-67.
3. Lee, S.Y., S.I. Kim, and M.E. Choi, Therapeutic targets for treating fibrotic kidney diseases. Transl Res, 2015. 165(4): p. 512-30.
4. Rockey, D.C., P.D. Bell, and J.A. Hill, Fibrosis--a common pathway to organ injury and failure. N Engl J Med, 2015. 372(12): p. 1138-49.
5. Cernaro, V., et al., New therapeutic strategies under development to halt the progression of renal failure. Expert Opin Investig Drugs, 2014. 23(5): p. 693-709.
6. Mutsaers, H.A.M., et al., Chronic kidney disease and fibrosis: the role of uremic retention solutes. Frontiers in Medicine, 2015. 2.
7. Eddy, A.A. and A.B. Fogo, Plasminogen activator inhibitor-1 in chronic kidney disease: evidence and mechanisms of action. J Am Soc Nephrol, 2006. 17(11): p. 2999-3012.
8. Inoue, T., et al., The contribution of epithelial-mesenchymal transition to renal fibrosis differs among kidney disease models. Kidney Int, 2015. 87(1): p. 233-8.
9. Poosti, F., et al., Precision-cut kidney slices (PCKS) to study development of renal fibrosis and efficacy of drug targeting ex vivo. Dis Model Mech, 2015.
10. de Graaf, I.A., et al., Preparation and incubation of precision-cut liver and intestinal slices for application in drug metabolism and toxicity studies. Nat Protoc, 2010. 5(9): p. 1540-51.
11. Westra, I.M., et al., Precision-cut liver slices as a model for the early onset of liver fibrosis to test antifibrotic drugs. Toxicol Appl Pharmacol, 2014. 274(2): p. 328-38.
12. De Kanter, R., et al., Drug-metabolizing activity of human and rat liver, lung, kidney and intestine slices. Xenobiotica, 2002. 32(5): p. 349-62.
13. van de Bovenkamp, M., et al., Liver slices as a model to study fibrogenesis and test the effects of anti-fibrotic drugs on fibrogenic cells in human liver. Toxicol In Vitro, 2008. 22(3): p. 771-8.
14. Mutsaers, H.A., et al., Uremic toxins inhibit renal metabolic capacity through interference with glucuronidation and mitochondrial respiration. Biochim Biophys Acta, 2013. 1832(1): p. 142-50.
15. Nomura, M., et al., Developmental expression of renal organic anion transporters in rat kidney and its effect on renal secretion of phenolsulfonphthalein. Am J Physiol Renal Physiol, 2012. 302(12): p. F1640-9.
16. Brown, C.D., et al., Characterisation of human tubular cell monolayers as a model of proximal tubular xenobiotic handling. Toxicol Appl Pharmacol, 2008. 233(3): p. 428-38.
17. Margaillan, G., et al., Quantitative profiling of human renal UDP-glucuronosyltransferases and glucuronidation activity: a comparison of normal and tumoral kidney tissues. Drug Metab Dispos, 2015. 43(4): p. 611-9.
18. Pusztaszeri, M.P., W. Seelentag, and F.T. Bosman, Immunohistochemical expression of endothelial markers CD31, CD34, von Willebrand factor, and Fli-1 in normal human tissues. J Histochem Cytochem, 2006. 54(4): p. 385-95.
19. Zeisberg, E.M., et al., Fibroblasts in kidney fibrosis emerge via endothelial-to-mesenchymal transition. J Am Soc Nephrol, 2008. 19(12): p. 2282-7.
20. Herman-Edelstein, M., et al., Dedifferentiation of immortalized human podocytes in response to transforming growth factor-beta: a model for diabetic podocytopathy. Diabetes, 2011. 60(6): p. 1779-88.
21. van Roeyen, C.R., et al., Induction of progressive glomerulonephritis by podocyte-specific overexpression of platelet-derived growth factor-D. Kidney Int, 2011. 80(12): p. 1292-305.
22. Miceli, I., et al., Stretch reduces nephrin expression via an angiotensin II-AT(1)-dependent mechanism in human podocytes: effect of rosiglitazone. Am J Physiol Renal Physiol, 2010. 298(2): p. F381-90.
23. Hinz, B., The myofibroblast: paradigm for a mechanically active cell. J Biomech, 2010. 43(1): p. 146-55.
24. Strutz, F. and M. Zeisberg, Renal fibroblasts and myofibroblasts in chronic kidney disease. J Am Soc Nephrol, 2006. 17(11): p. 2992-8.
25. Border, W.A. and N.A. Noble, Transforming growth factor beta in tissue fibrosis. N Engl J Med, 1994. 331(19): p. 1286-92.
26. Eddy, A.A., Overview of the cellular and molecular basis of kidney fibrosis. Kidney Int Suppl (2011), 2014. 4(1): p. 2-8.
27. Lin, S.L., et al., Bone marrow Ly6Chigh monocytes are selectively recruited to injured kidney and differentiate into functionally distinct populations. J Immunol, 2009. 183(10): p. 6733-43.